2024 Road Safety & Simulation Conference
Improving Decisions Through Safety and Simulation Tools
Lexington, KY, USA
October 28-31, 2024

Merging Multi-antenna GPS Data for Vehicle Pose Estimation

Xinyu Cao[1], Sean Brennan

Mechanical Engineering, The Pennsylvania State University, University Park, PA,16802, USA, xfc5113@psu.edu
Mechanical Engineering, The Pennsylvania State University, University Park, PA,16802, USA, sbrennan@psu.edu

Abstract

In measuring, evaluating, and controlling the motion of a vehicle, no data is more important than its position and velocity, and on modern vehicle systems this is primarily derived via the Global Positioning System (GPS). There have been many studies on sensor calibration in autonomous vehicles, and significant progress has been made in sensor performance, fusing sensor information, and reducing sensor costs to where most production vehicles today contain at least one GPS system in-vehicle, and often with several others in phones and similar smart devices. However, the calibration accuracy of vehicle position, particularly when differential corrections are used to obtain centimeter-level precision, is difficult to establish. Positioning errors can emerge in correcting data from the antenna position measurements in Earth-fixed coordinates, to/from the position of the antenna on the vehicle in vehicle-fixed coordinates to/from the position of the vehicle path's center-of-motion or center of gravity. Many antenna systems, particularly those used for research or involving multiple antenna systems, necessarily include positioning errors caused by installation or calibration of baseline distances, and there is no standard procedure for the calibration methods when using multiple Global Positioning System (GPS) units when those units are being fused to obtain the full vehicle pose including positions and orientations of the vehicle. This article proposes a systematic calibration method for the installation of multiple GPS units. The process is demonstrated for a road-mapping vehicle that uses GPS data collection with multiple antennas and with time segments of data collected during vehicle motion. The calibration uses Gram–Schmidt orthonormalization to eliminate the errors caused by installation limitations and offsets to solve the inherent defects and changes in GPS measurement caused by installation. The coordinate transformation-based algorithm is tested in this paper to precisely estimate a vehicle's position and orientation by integrating multiple GPS units, offering a promising and automation solution for applications such as autonomous vehicles and intelligent transportation systems in real-world applications where precise and reliable pose estimation is crucial.

Keywords: sensor calibration, sensor fusion, vehicle localization, advanced mapping system, Global Positioning System

[1] * Corresponding author. Tel.: +1-206-953-8785;
E-mail address: xfc5113@psu.edu

1. Introduction

Accurate vehicle pose estimation is critical for a wide range of applications in the fields of autonomous driving, vehicle navigation systems, vehicle mapping, and road safety evaluations. Precise measurement of position and orientation is crucial as it allows for more accurate vehicle localization and motion prediction [1]. Modern vehicle pose estimation has relied heavily on a combination of sensors including Global Positioning System (GPS), inertial measurement units (IMUs), inertial navigation system (INS), and optical sensors [2].

These systems have provided foundational capabilities especially for driver-assist and automation systems for vehicles, and numerous methods have been developed to enhance the accuracy of pose estimation via GPS due to its widespread availability and robustness in providing absolute positioning data. For instance, Lee et al. have explored the integration of a single GPS antenna system with IMU to enhance the accuracy and reliability of the localization methods for Unmanned Ground Vehicles [3]. Similarly, Li et al. developed the tightly-coupled single-frequency multi-GNSS RTK/MEMS-IMU integration to provide precise and continuous positioning solutions in urban environments [4]. Another study by Cai et al. focused on integrating multi-antenna GPS with IMUs for precise yaw angle and attitude determination for vehicle-mounted mapping systems [5].

Despite significant advancements in sensor performance and sensor fusion, GPS accuracy and reliability can be significantly affected by environmental factors, sensor limitations, the dynamic nature of vehicle movements, and an often-overlooked factor: errors caused by the installation and calibration of position offsets of antennas on the vehicle. There is no standard procedure for multiple GPS units used to determine a full vehicle pose, including the position and the orientation of the vehicle. The motivation for developing a new vehicle pose estimation method stems from the critical need for enhanced accuracy of vehicle localization and navigation.

This paper addresses these challenges by proposing a systematic calibration method tailored for the installation of multiple GPS units on mapping vehicles. Robust and centimeter-level Real Time Kinematic (RTK) service is provided to enhance the accuracy of each GPS unit [6]. By leveraging Gram–Schmidt orthonormalization [7], the method effectively eliminates installation errors, mitigating the inherent defects and variations in GPS measurements caused by installation constraints.

The coordinate transformation-based algorithm introduced in this study precisely estimates a vehicle's position and orientation by integrating data from multiple GPS units. Tested under real-world conditions, this method demonstrates its potential to provide reliable and precise pose estimation. Such advancements are crucial for applications in autonomous vehicles and intelligent transportation systems where accurate and dependable vehicle pose information is vital.

The remainder of this paper is structured as follows: Section II details the proposed calibration method and geometric transformation-based algorithm for vehicle pose estimation. Section III presents the experimental results and analysis. Section IV discusses the findings and their implications. Finally, conclusions are discussed in Section V.

2. Methodology

2.1 System Overview

In this paper, we proposed a vehicle pose estimation method based on multi-GPS units. For pose estimation, multi-unit GPS mountings benefit from the widest separation of antennas possible without blocking GPS coverage. In this work, three GPS antennas are mounted at distinct extremities of the vehicle's roof to maximize spatial separation, which in turn maximizes the precision of positional and orientation data. A high rigidity low thermal expansion stainless steel frame connects the antennas and sensors together, largely removing the small but non-negligible flex that occurs in typical vehicle mountings. A Differential Global Positioning System (DGPS) is set up to provide RTK positioning service to the GPS units which provides real-time positioning accuracy down to centimeter or even millimeter level. All three GPS units are interfaced with an Ubuntu machine installed in the vehicle, utilizing the Robot Operating System (ROS) for enhanced interoperability and real-time data handling. Custom-developed ROS packages are utilized to collect GPS data. Once collected, the data is processed in MATLAB using specially designed calibration algorithms to synchronize data and then correct the installation error of the GPS units to estimate the origin and orientations of the vehicle through coordinates transformation.

2.2 Coordinate System

The following coordinate systems are defined to illustrate vehicle pose estimation algorithms:

- Local East, North, Up (ENU) coordinate system (E): It has an origin (O_E) at the base station of the DGPS system, with X-axis pointing east (e_X), the Y-axis system pointing North (e_Y), and the Z-axis pointing up (e_Z), which is defined in ISO-8855 [8].
- Vehicle coordinate system (V): The coordinate system of the vehicle with X-axis pointing forward (v_X), the Y-axis system pointing left (v_Y), and the Z-axis pointing up (v_Z). The origin (O_V) of the vehicle coordinate system is located at the geometric midpoint of the rear axle.[9]
- GPS coordinate system (G): The coordinate system formed with three GPS antennas, with origin located by the user's choice. In this work, it is located at the position of the rear right GPS antenna. Its orientations are introduced in the following sections.
- Virtual GPS coordinate system ($\hat{G}$): A virtual coordinate system has the same orientations as the vehicle coordinate system while its origin is located at the rear right GPS antenna.

2.3 Data Collection and Preprocessing

This study focuses on developing a method to estimate the vehicle pose using GPS data from three GPS units. The installation of the three GPS units is shown in Figure 1, three GPS antennas are mounted at distinct corners of the vehicle's roof to maximum spatial separation to derive precise positional and orientation data. Each GPS unit was configured to receive Global Positioning Fix Data (GPGGA) at a frequency of 10 Hz, which includes latitude, longitude, altitude, time stamp, speed, GPS quality indicator, and the time since the last DGPS update. All three GPS units are interfaced with an Ubuntu 20.04 machine, and Robot Operating System (ROS) is running on the machine to record data from all three GPS units.

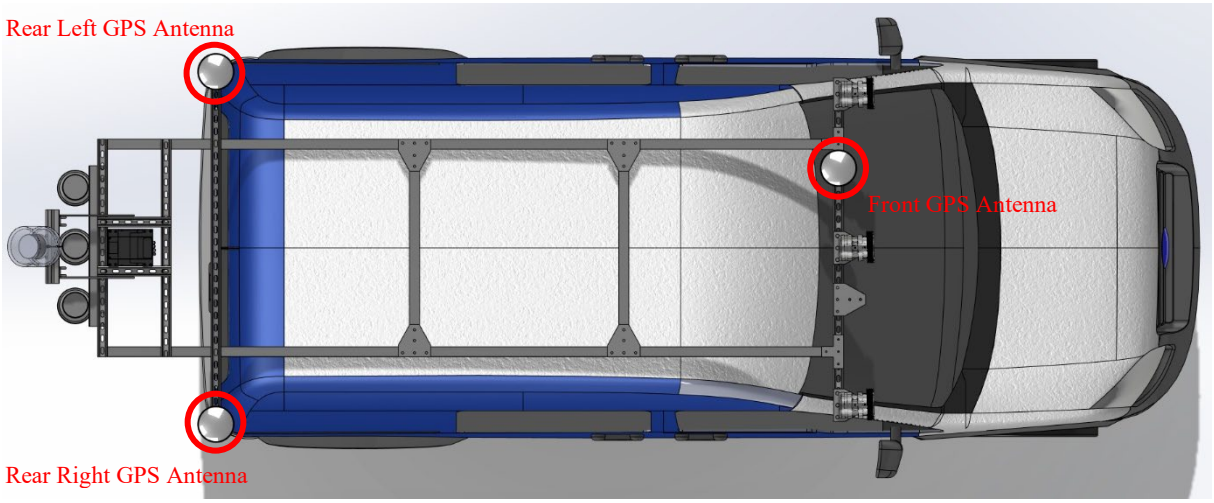

Figure 1: The installation of three GPS units on the vehicle

To improve the accuracy of the GPS data, a Networked Transport of RTCM via Internet Protocol (NTRIP) system (2 micro-second accuracy) was built to stream RTK corrections from the reference base station to a GPS rover to achieve millimeter-level positioning accuracy, which is shown in Table 1. In our study, SparkFun Top106 GNSS antenna is used for both the base station and GPS rovers. The Penn State LTI Test Track base station was used in the system, and all data were collected within one kilometer of the base station.

Table 1. GPS units' standard error (1-sigma recorded over 15 minutes)

GPS unit	Standard error of GPS data without RTK [m]	Standard error of GPS data with RTK fixed [m]
Front GPS	[0.4598 0.1082 0.7850]	[0.0025 0.0023 0.0040]
Rear Left GPS	[0.5011 0.1328 1.0921]	[0.0018 0.0024 0.0052]
Rear Right GPS	[0.1408 0.3503 0.9297]	[0.0023 0.0026 0.0042]

Once data was collected, the data was first cleaned to remove unlocked data, which indicates that only GPS data with RTK fixed are to be used to estimate the vehicle pose. The filtered GPS data are trimmed and interpolated to ensure all recordings from three GPS units are exactly time-synchronized. This preprocessing step is critical for the accuracy and reliability of the vehicle pose estimations in later stages of the vehicle pose estimation detailed in the following sessions.

2.4 Vehicle Pose Estimation

The problem of estimating the vehicle pose is equivalent to estimating the origin of the vehicle coordinate system, and the orientation (roll, pitch, and yaw) of the vehicle coordinate system under the local ENU coordinate system. Ideally, directly installing the GPS/INS system at the midpoint of the rear axle is the easiest solution; however, this is also an impossible solution in a real application and thus one observes that the vehicle pose cannot be directly measured in nearly all vehicle applications. Therefore, a calibration-based method is necessary to estimate vehicle pose by constructing a reference coordinate system and determining the coordinate transformation between the vehicle coordinate system and the reference coordinate system.

2.4.1 Construct Reference Coordinate System

The GPS coordinate system G is chosen as the reference coordinate system whose origin is placed at the position of the rear right GPS antenna. The main calibration task in constructing a reference coordinate system is to establish its orthonormal basis. Gram–Schmidt orthonormalization is used to construct the orthonormal basis B_G for the rear GPS coordinate system. To explain, by construction the origin of the rear GPS coordinate system is positioned at the rear right GPS antenna. Taking the vector $\boldsymbol{v_{O\to L}}$ as the first vector of the orthogonal basis, $\boldsymbol{g_1}$, which is the vector pointing from the origin to the rear left GPS antenna, one can identify the direction of the Y-axis of G. One can next compute the vector pointing from the origin to the front GPS antenna, which is denoted as $\boldsymbol{v_{O\to F}}$. Since $\boldsymbol{v_{O\to L}}$ and $\boldsymbol{v_{O\to F}}$ are two vectors on the GPS plane, the normal vector of the GPS plane is given by:

$$\boldsymbol{n_G} = \boldsymbol{v_{O\to F}} \times \boldsymbol{v_{O\to L}} \tag{1}$$

which is taken as the second vector of the orthogonal basis, $\boldsymbol{g_2}$, representing the direction of the Z-axis of G. To construct an orthogonal basis, all the vectors should be unit vectors, thus, must normalize vectors $\boldsymbol{g_1}$ and $\boldsymbol{g_2}$ to obtain the unit vectors along Y_G and Z_G axis, which are given by:

$$\boldsymbol{g_Y} = \frac{\boldsymbol{g_1}}{\|\boldsymbol{g_1}\|} \tag{2}$$

$$\boldsymbol{g_Z} = \frac{\boldsymbol{g_2}}{\|\boldsymbol{g_2}\|} \tag{3}$$

Thus, the third vector that identifies the direction of X-axis is given by:

$$\boldsymbol{g_X} = \boldsymbol{g_Y} \times \boldsymbol{g_Z} \tag{4}$$

And the orthonormal basis for the rear GPS coordinate system is given by:

$$B_G = \{\boldsymbol{g_X} \quad \boldsymbol{g_Y} \quad \boldsymbol{g_Z}\} \tag{5}$$

2.4.2 Determine the transformation between two coordinate systems

Ideally, considering the position of the rear right GPS antenna as the origin, if all three GPS antennas are perfectly installed, namely with two rear GPS antennas mounted exactly along Y_V and the front GPS antenna aligned exactly with the rear right antenna along X_V, this forces the antenna-specific GPS coordinate system G to have the same orientation as the vehicle coordinate system V. However, in actual situations, the orientations of the two coordinate systems are almost never aligned due to installation errors, antenna design factors, and even vehicle loading conditions which change roll and pitch. Therefore, the transformation between G and V needs to be determined, including the rotation transformation and the translational transformation.

2.4.3 Determine the rotation transformation

To find the orientation of the vehicle coordinate system, an experiment involving gathering GPS and encoder data as the vehicle travels in a straight lane was set up. To eliminate geometric effects caused by road superelevation or grade, the vehicle drives along a straight road segment to collect initial dataset, then reverses its direction to carefully drive on the same segment for additional data collection. Each cycle of forward and reverse travel constitutes a complete dataset. This experiment was repeated three times to ensure the repeatability and robustness of the data collected.

Since the vehicle travels in approximately a straight line, the movement trajectories of the three GPS units align, all oriented in the direction of the vehicle's forward movement which is, by construction, the X-axis of the vehicle coordinate system. In each data set, the moving trajectories from three GPS units are computed and averaged separately for both forward and reverse directions to obtain the first vector of the orthonormal basis of a vehicle coordinate system, $\boldsymbol{v_1}$, which points to the X direction of the vehicle coordinate system.

If the GPS units are installed without any error, the vector representing the Z direction would be perpendicular to both GPS plane and the road surface. This implies that in the ENU coordinate system, the representation of the vehicle's orientation along Z-axis would remain consistent regardless of the direction of travel along the same road

segment. However, installation errors introduce directional biases which will produce different normal vectors for each travel direction, varying with the vehicle's orientation. For vectors from two opposite directions, the errors they contained are also opposite. Therefore, averaging these vectors yields a vector perpendicular to the road surface. In our case, the normal vectors from two directions are denoted as $\boldsymbol{n_{G-F}}$ and $\boldsymbol{n_{G-R}}$ respectively, and the vector that is perpendicular to the current road surface is given by:

$$\boldsymbol{n_{road}} = \frac{\boldsymbol{n_{G-F}} + \boldsymbol{n_{G-R}}}{2} \tag{6}$$

which is taken as the second vector of the orthonormal basis, $\boldsymbol{v_2}$, representing the direction of the Z-axis. And then, the third vector that represents the direction of the Y axis is given by

$$\boldsymbol{v_3} = \boldsymbol{v_2} \times \boldsymbol{v_1} \tag{7}$$

Normalize all three vectors and we can construct the orthonormal basis B_V of the vehicle coordinate system,

$$\boldsymbol{v_X} = \frac{\boldsymbol{v_1}}{\|\boldsymbol{v_1}\|} \tag{8}$$

$$\boldsymbol{v_Y} = \frac{\boldsymbol{v_3}}{\|\boldsymbol{v_3}\|} \tag{9}$$

$$\boldsymbol{v_Z} = \frac{\boldsymbol{v_2}}{\|\boldsymbol{v_2}\|} \tag{10}$$

$$B_V = \{\boldsymbol{v_X} \quad \boldsymbol{v_Y} \quad \boldsymbol{v_Z}\} \tag{11}$$

which only represents the orientation of the vehicle coordinate system on this specific straight segment.

With the reference coordinate system and vehicle's orthonormal basis defined, we can construct two rotation matrices R_{EG} and R_{EV}, respectively represent the transformations from the GPS and vehicle coordinate systems to the ENU coordinate system, where:

$$R_{EG} = [\boldsymbol{g_X}^T \quad \boldsymbol{g_Y}^T \quad \boldsymbol{g_Z}^T] \tag{12}$$

$$R_{EV} = [\boldsymbol{v_X}^T \quad \boldsymbol{v_Y}^T \quad \boldsymbol{v_Z}^T] \tag{13}$$

Then, the roll, pitch and yaw angle of the vehicle can be extracting from the rotation matirx R_{EV}, and the rotation transformation from the GPS coordinate system to the vehicle coordinate system is given by:

$$R_{VG} = R_{VE}R_{EG} = (R_{EV})^{-1}R_{EG} \tag{14}$$

which indicates that at any road section, one can calculate the vehicle orientations by calculating the orientations of the GPS coordinate system and applying the calculated rotation matrix R_{VG}, as shown in equation below:

$$R_{VE} = R_{VG}R_{GE} = R_{VG}(R_{EG})^{-1} \tag{15}$$

2.4.4 Determine the translational transformation

Up to now, the focus has been to derive the rotation transformation between the GPS coordinate system and the vehicle coordinate system. Still missing is the translational transformation between these two coordinate systems, in other words, the relative position of the vehicle origin and the rear GPS antenna. To accurately obtain this relative position, a virtual GPS coordinate system $\hat{G}$ is established by applying the rotation matrix R_{VG} to the GPS coordinate system G, and the transformation between $\hat{G}$ and E is given by:

$$T_{E\hat{G}} = \begin{bmatrix} R_{EG}R_{GV} & O_G^E \\ 0 \quad 0 \quad 0 & 1 \end{bmatrix} = \begin{bmatrix} R_{EV} & O_G^E \\ 0 \quad 0 \quad 0 & 1 \end{bmatrix} \tag{16}$$

The virtual GPS coordinate system has the same orientations as the vehicle coordinate system and shares the origin with the GPS coordinate system, which implies one can measure the relative position with tape measure to obtain the measurement of the vehicle origin's relative position to the rear GPS antenna, which will serve as the initial estimate for the vehicle origin's position. Thus, the homogeneous transformation between $\hat{G}$ and V can be written as:

$$\tilde{T}_{\hat{G}V} = \begin{bmatrix} I_{3\times3} & \tilde{P}_{G-V} \\ 0 \quad 0 \quad 0 & 1 \end{bmatrix} \tag{17}$$

where $I_{3\times3}$ denotes a 3-by-3 identity matrix and $\tilde{P}_{G-V}$ denotes the relative position of the vehicle origin to the rear right GPS antenna in the virtual GPS coordinate system, which is the initial estimate based on the hand measurements. The transformation from the vehicle coordinate system to the ENU coordinate system, using the initial estimate, is given by:

$$\tilde{T}_{EV} = T_{E\hat{G}}\tilde{T}_{\hat{G}V} \tag{18}$$

Afterward, a special region is measured and marked on the pavement with lane marking tapes, and the mapping van is parked in two opposite directions along the yellow lane maker, ensuring that both rear wheels are strictly within this taped region, as shown in Figure 2. Once the mapping vehicle is parked at the right position, static GPS data is collected from three GPS units, with three sets of data gathered for each direction.

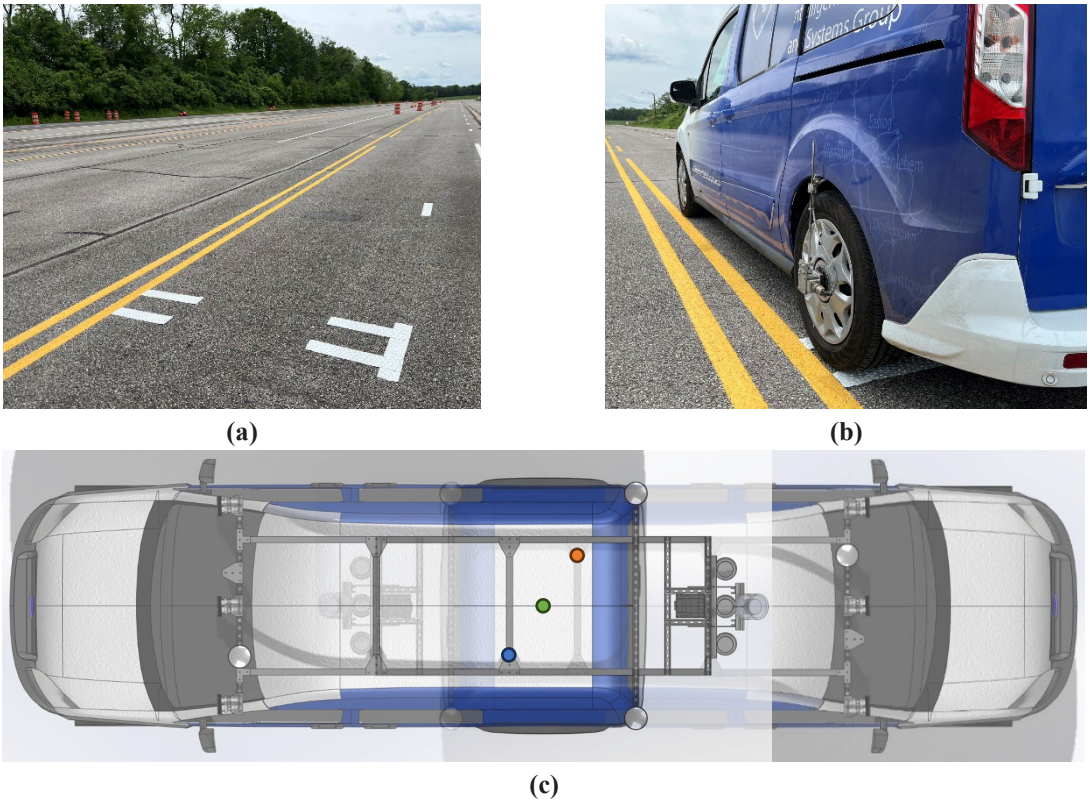

Figure 2: A taped region was used for vehicle origin estimation. (a) region made with lane marking tapes, (b) the mapping vehicle was parked with both rear wheels positioned within the taped region, (c) collect GPS data from two opposite directions

The blue and orange dots represent the vehicle origin calculated using initial estimate $\tilde{P}_{G-V}$ from two different datasets, with the vehicle headed in two opposite directions, respectively. The green dot is the final estimated vehicle origin obtained by averaging the coordinates of the blue and orange dots calculated in all six data sets to correct the error caused by the hand measurements, the result is given by:

$$\bar{O}_V^E = \frac{1}{m}\sum_{i=1}^{m} \tilde{T}_{EV\,i} O_V^V \tag{19}$$

Where O_V^V denote the vehicle origin in the vehicle coordinate system, m is the total number of the data sets, $\tilde{T}_{EV\,i}$ is the hypothesized transformation for the current data set, $\bar{O}_V^E$ denotes the expression of the averaged vehicle origin in the ENU coordinate system. Afterward, transform the averaged vehicle origin back to the virtual GPS coordinate system in each data set and average the transformed vehicle origins to find the aveaged vehicle origin in the virtual GPS coordinate system, which is given by:

$$\bar{O}_V^{\hat{G}} = T_{\hat{G}E}\bar{O}_V^E = (T_{E\hat{G}})^{-1}\bar{O}_V^E \tag{20}$$

And then, the relative position of the vehicle origin to the rear right GPS antenna in X and Y directions can be obtained:

$$\Delta x = \bar{O}_{V,X}^{\hat{G}} \tag{21}$$

$$\Delta y = \bar{O}_{V,Y}^{\hat{G}} \tag{22}$$

where $\bar{O}_{V,X}^{\hat{G}}$ and $\bar{O}_{V,Y}^{\hat{G}}$ represents the expression of the X and Y coordinates of the vehicle's origin in the virtual GPS coordinate system.

To find the relative position in the Z direction, a survey GPS antenna was used to measure the positions of the four corners of the taped area. After this, the central position of the area P_C can be calculated. Additionally, the distance from this central point to the XY-plane of the virtual GPS coordinate system can be determined by projecting the

P_C to the plane. By subtracting the tire's radius, the relative distance in Z direction can be derived, which is given by

$$\Delta z = d_c - r_{wheel} \tag{23}$$

where d_c is the distance from the center point to the XY-plane of $\hat{G}$, and r_{wheel} denotes the radius of the rear wheel. The final estimation of the relative position of the vehicle origin to the rear right GPS antenna is shown in Table 2.

Table 2: The Relative Position of the Vehicle Origin to the Rear Right GPS Antenna

Relative Distance	Estimated value [m]	Standard error [m]
Δx	-0.6552	0.0045
Δy	-0.7422	0.0086
Δz	1.6865	0.0025

3. Analysis and Results

Since the actual position and orientation of the vehicle cannot be directly obtained, one is generally unable to compare the estimated vehicle pose with the ground-truth directly. With mapping vehicles, the consistency of external sensor measurements measuring the same feature can serve as a surrogate; this itself is a difficult process and one that introduces significant calibration challenges. For simplicity, this section focuses on the repeatability and statistical variance of the proposed method from testing on different types of roads.

First, another set of data was collected at the taped region mentioned in section 3.1.3 to check the variation of the estimated vehicle origin, which is shown in Table 3.

Table 3: The Estimated Vehicle Origin at the Taped Region

Vehicle Origin	Estimated value [m]	Standard error [m]
x	375.9512	0.0034
y	73.5288	0.0087
z	-10.2233	0.0026

Afterward, as shown in Figure 3, data collection was conducted at the Penn State LTI Test Track over different types of road sections to evaluate the consistency, including a straight road segment, a curved road with a constant radius, and a complete standard route that included both straight and curved sections.

(a) **(b)**

Figure 3: Data collection example. (a) a straight road segment, (b) curved road with constant radius

In each dataset, the roll, pitch, and yaw angles are calculated to represent the variations caused by different road sections, as shown in Figure 4, the estimated vehicle orientations as it traverses different road sections. Figure 4(a) shows that when the vehicle is traveling along a straight road segment, both roll and pitch angles show high-frequency variations, indicating the vehicle's frequent adjustments in response to uneven road surfaces or changes in road elevation. The yaw angle changes smoothly with some periodic deviations, resulting from the small adjustments made by the driver to maintain a straight line. The yaw angle from Figure 4(b) demonstrates a consistent increase in the yaw rate of 0.0552 ± 0.0088 rad/s, consistent with the vehicle traveling on a curved road with a constant radius.

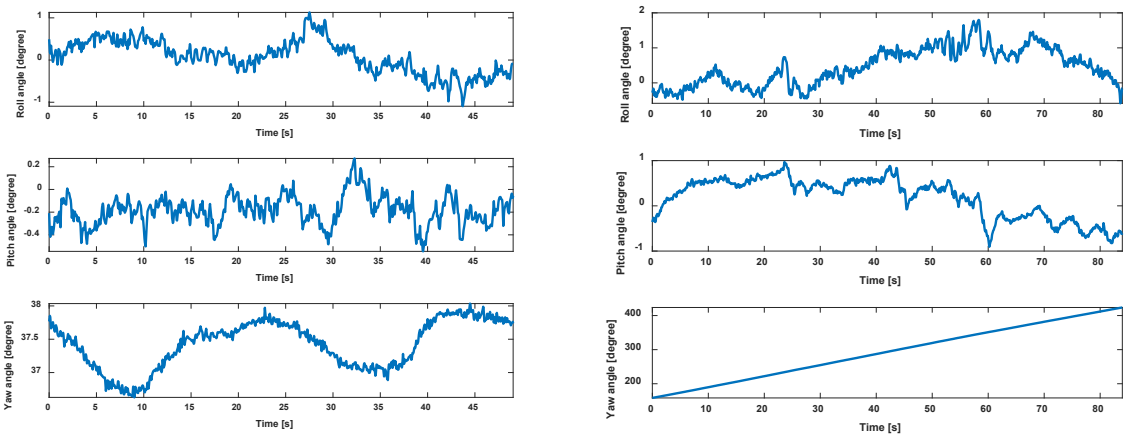

(a) (b)

Figure 4: Vehicle estimated orientation tracking. (a) at straight road segment, (b) at curved road with constant radius

Additionally, two calibrated encoders, in conjunction with the low-speed kinematic model, were used to determine whether the estimated vehicle origin aligns with the theoretical origin, the midpoint of the rear axle.

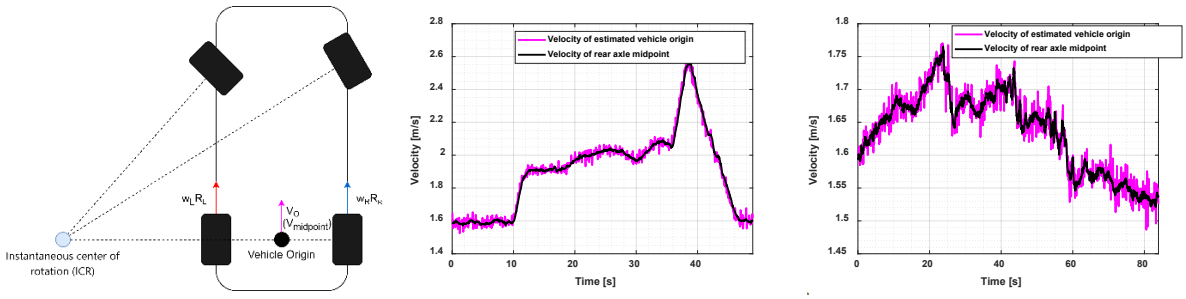

(a) (b) (c)

Figure 5: Vehicle motion about the ICR. (a) vehicle kinematic model, (b) vehicle velocity on the straight road segment, (c) vehicle velocity on the curved road section with constant radius

Figure 5 shows the vehicle motion about the instantaneous center of rotation (ICR), where point O_V is the center gravity point of the vehicle located at the midpoint of the rear axle. According to ICR's definition, it is the point in the plane in which all other points are rotated at a specific instant of time. For the low-speed kinematic four-wheel vehicle model, the slip angles of all four tires are assumed to be zero, which indicates the encoder-predicted velocity of the midpoint of the rear axle is given by:

$$V_{midpoint} = \frac{V_{RL}+V_{RR}}{2} \qquad (23)$$

Subplots (b) and (c) in Figure 5 show a strong correlation between the velocities of the estimated vehicle origin and the rear axle midpoint throughout the entire duration. This close correlation suggests that the estimation algorithms for the vehicle pose is effectively capturing the real movements of the vehicle for both straight and curved road.

For the complete regular route section, the vehicle traveled the same route three times, starting and ending at the same points each time, as shown in Figure 6. Data was collected for three laps to verify the consistency of the vehicle's pose estimation. The route included straight segments, a lane change area, and curved roads with different radii and surface inclinations. These different sections of the route can comprehensively demonstrate the system's response and performance when encountering various road conditions.

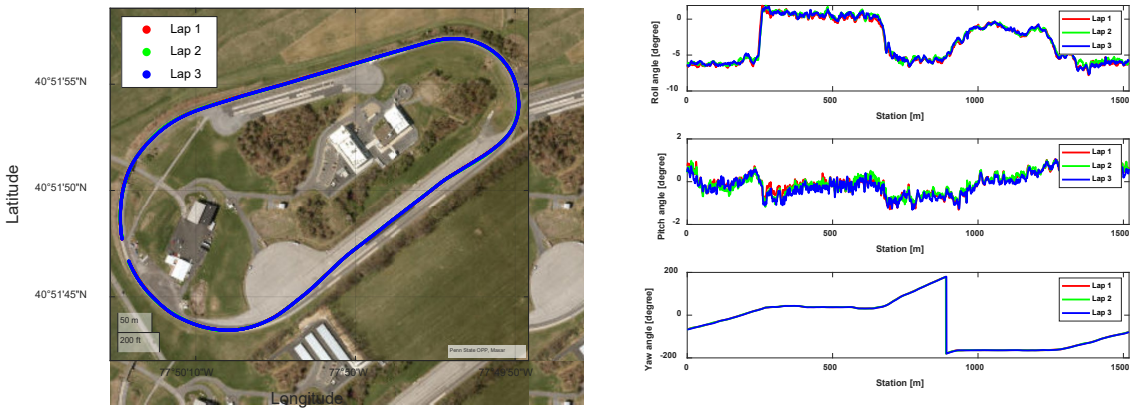

(a) (b)

Figure 6: Vehicle pose tracking on the regular route section. (a) vehicle origin tracking across all three laps, (b) vehicle orientation tracking across all three laps

Compared to position estimation, the results of orientation estimation can be more intuitively represented, as shown in Figure 6(b). This plot shows relatively consistent patterns across all three laps, with slight deviations likely due to road imperfections or slight variations in driving. The roll angles are generally close to zero, indicating minimal lateral tilt, which is ideal for typical driving scenarios. The pitch angles display more variability compared to roll angles, yet they follow a similar trend across the three laps. This indicates a consistent response to the longitudinal profile of the road, such as superelevation or road grade. Yaw angles from all three laps are also highly aligned, the sharp decline is due to the angle switching to a negative value after exceeding 180 degrees. The increasing trend across all laps reflects the vehicle navigating through a series of continuous turns or a circular path, consistent with the geometry of a closed-loop track. By integrating the estimation across all three laps and calculating the average standard deviations for all stations along the path, vehicle's roll, pitch, and yaw angles have standard deviations of 0.0049°, 0.0029°, and 0.0185°, respectively. These observations indicate an accurate and reliable vehicle pose estimation system capable of maintaining consistent orientations even when subjected to the same road conditions repeatedly.

4. Discussion

Our study proposes a systematic calibration method that employs Gram–Schmidt orthonormalization to eliminate installation limitations and offsets. This method provides a structured approach to integrating multiple GPS units, thereby improving the accuracy of vehicle position and orientation estimation. By integrating data from multiple GPS units, the proposed method provides a robust solution that mitigates the inherent defects and variations in GPS measurements caused by installation constraints and errors. This improvement is crucial for real-world applications, such as mapping vehicles, autonomous vehicles, and intelligent transportation systems, where precise and reliable pose estimation is essential.

The experimental results demonstrate that merging data from multiple antennas significantly enhances the accuracy of vehicle pose estimation. One can observe, for example, that the statistical accuracy of the calibration method in position is functionally at the theoretical limit; namely, the 1-sigma error for the 3-antenna merged position is approximately the 1-sigma error of a single antenna divided by square-root of 3. By employing a coordinate transformation-based algorithm, the method effectively aligns the vehicle's coordinate system, resulting in precise position and reliable orientation estimates. This is particularly important for applications requiring high precision, such as autonomous driving and advanced mapping systems.

5. Conclusions

The accuracy of vehicle position and orientation measurements is critical for mapping and autonomous vehicles. While significant progress has been made in sensor performance and data fusion, errors caused by sensor installation are often overlooked. This paper presents a straightforward and effective approach to vehicle pose estimation by merging multi-antenna GPS data. The proposed systematic calibration method employs Gram–

Schmidt orthonormalization to eliminate installation-induced errors, significantly improving the accuracy of vehicle position and orientation estimation.

The proposed method demonstrated significant accuracy in vehicle pose estimation. The standard deviation for vehicle position estimations in the X, Y, and Z axes was measured at 0.0034 m, 0.0087 m, and 0.0026 m, respectively. Additionally, the standard deviation for orientation were 0.0049° in roll, 0.0029° in pitch, and 0.0185° in yaw. These results were achieved across various scenarios, including straight road segments, lane change areas, and curved roads with different radii and surface inclinations, validating the accuracy and reliability of our approach. The systematic calibration and data fusion method successfully mitigated the errors introduced by sensor misalignment, proving its effectiveness in real-world conditions. These findings highlight the importance of addressing installation-induced errors and validate the proposed method's capability to enhance the precision of vehicle pose estimation.

Overall, this research demonstrates that merging multi-antenna GPS data is an effective strategy for achieving high-precision vehicle pose estimation. The accuracy demonstrated by the proposed method marks a pivotal step toward the development of reliable and efficient autonomous navigation systems. Future research building on these findings can pave the way for even more advanced and resilient vehicle pose estimation techniques, contributing to the broader field of autonomous driving and intelligent transportation systems.

6. Acknowledgment

This material is based upon work supported by PennDOT and USDOT, via the ADS Grant “Safe Integration of ADS Vehicles into Work Zones (PennDOT)”. The findings here are those of the authors only, and do not represent endorsement by the sponsors.

7. References

[1] T. G. R. Reid et al., “Localization Requirements for Autonomous Vehicles,” SAE International Journal of Connected and Automated Vehicles, vol. 2, no. 3, Sep. 2019, doi: https://doi.org/10.4271/12-02-03-0012.

[2] H. Chen, W. Wu, S. Zhang, C. Wu, and R. Zhong, “A GNSS/LiDAR/IMU Pose Estimation System Based on Collaborative Fusion of Factor Map and Filtering,” Remote Sensing, vol. 15, no. 3, p. 790, Jan. 2023, doi: https://doi.org/10.3390/rs15030790.

[3] Jae Un Lee, D.-H. Park, and J.-H. Won, “A Localization Method with UKF/MAF for a Single Antenna GNSS/IMU Integration of Autonomous Unmanned Ground Vehicle,” Oct. 2022, doi: https://doi.org/10.1109/sdf55338.2022.9931952.

[4] T. Li, H. Zhang, Z. Gao, Q. Chen, and X. Niu, “High-Accuracy Positioning in Urban Environments Using Single-Frequency Multi-GNSS RTK/MEMS-IMU Integration,” Remote Sensing, vol. 10, no. 2, p. 205, Jan. 2018, doi: https://doi.org/10.3390/rs10020205.

[5] X. Cai, H. Hsu, H. Chai, L. Ding, and Y. Wang, “Multi-antenna GNSS and INS Integrated Position and Attitude Determination without Base Station for Land Vehicles,” Journal of Navigation, vol. 72, no. 2, pp. 342–358, Sep. 2018, doi: https://doi.org/10.1017/s0373463318000681.

[6] M. Shao and X. Sui, "Study on Differential GPS Positioning Methods," 2015 International Conference on Computer Science and Mechanical Automation (CSMA), Hangzhou, China, 2015, pp. 223-225, doi: 10.1109/CSMA.2015.51.

[7] Å. Björck, “Numerics of Gram-Schmidt orthogonalization,” Linear Algebra and its Applications, vol. 197–198, pp. 297–316, Jan. 1994, doi: https://doi.org/10.1016/0024-3795(94)90493-6.

[8] “ISO 8855:2011.” ISO, www.iso.org/standard/51180.html.

[9] M. Meywerk, Vehicle dynamics. Chichester, West Sussex: Wiley, 2015.